

Freestanding HRP-GOx redox buckypaper as an oxygen-reducing biocathode for biofuel cell applications

Cosnier, Serge; Elouarzaki, Kamal; Bourourou, M.; Holzinger, M.; Le Goff, A.; Marks, Robert S.

2015

Elouarzaki, K., Bourourou, M., Holzinger, M., Le Goff, A., Marks R. S., & Cosnier S. (2015). Freestanding HRP-GOx redox buckypaper as an oxygen-reducing biocathode for biofuel cell applications. *Energy & environmental science*, in press.

<https://hdl.handle.net/10356/104725>

<https://doi.org/10.1039/C5EE01189B>

© 2015 The Royal Society of Chemistry. This is the author created version of a work that has been peer reviewed and accepted for publication by *Energy & Environmental Science*, The Royal Society of Chemistry. It incorporates referee's comments but changes resulting from the publishing process, such as copyediting, structural formatting, may not be reflected in this document. The published version is available at: [<http://dx.doi.org/10.1039/C5EE01189B>].

Downloaded on 13 Mar 2024 16:48:10 SGT

ARTICLE

Freestanding HRP–GOx redox buckypaper as oxygen-reducing biocathode for biofuel cell applications

Cite this: DOI: 10.1039/x0xx00000x

Received 00th January 2012,
Accepted 00th January 2012

DOI: 10.1039/x0xx00000x

www.rsc.org/

K. Elouarzaki ^{a,b}, M. Bourourou ^a, M. Holzinger ^a, Alan Le Goff ^a, R. S. Marks ^{b,c},
S. Cosnier ^{a*}

Horseradish peroxidase (HRP) was immobilized on redox buckypapers followed by electropolymerization of pyrrole-modified concanavalin A enabling the subsequent additional immobilization of the glycoprotein glucose oxidase (GOx). Biocatalytic buckypapers were formed using pyrene-modified 2,2'-Azino-bis(3-ethylbenzothiazoline-6-sulfonic acid) or Bis-Pyr-ABTS, a redox mediator, as a cross linker. ABTS-functionalized buckypaper enhances electron transfer of the bioelectrocatalytic reduction of hydrogen peroxide by HRP. Since H₂O₂ is produced during glucose oxidation by GOx in the presence of oxygen, the bienzymatic GOx-HRP biocathode achieves the complete reduction of oxygen into water. Clearly improved performance of the biocathode was obtained by using an improved biocompatible immobilization strategy, enabling the prevention of enzyme loss while, ensuring both diffusion of glucose and O₂ and the local production of H₂O₂. These freestanding flexible oxygen-reducing biocathodes can operate in physiological conditions and show a high onset potentials at 0.60(± 0.01) V. In the presence of glucose (5 mM), such biocathodes exhibit a stable current density output of 1.1(± 0.1) mA cm⁻² at 0.1 V under continuous one-hour discharge. Furthermore, a marked increase in lifetime was observed, the biocathode displaying 64 % of its initial electrocatalytic activity after 15 days.

Introduction:

Glucose biofuel cells are promising candidates for powering implantable biomedical devices by generating electricity out of body fluids¹. Several studies have reported different examples of implanted biofuel cells operating in vivo in various animals such as insects², snails³, clams⁴, lobsters⁵, rats⁶⁻¹⁰ and rabbits¹¹.

High-potential bioelectrocatalytic reduction of substrates such as oxygen or hydrogen peroxide by redox enzymes is an important challenge for the development of powerful biocathodes in enzymatic biofuel cell setups. Multicopper enzymes such as laccases^{12, 13} or bilirubin oxidases¹⁴⁻¹⁶ are generally used in biofuel cell design. However, they are known to not only lose activity in the presence of inhibitors such as chloride or urate ions, but they also do not demonstrate optimal

efficiency under physiological conditions, i.e. 5 mM glucose and 0.14 mM NaCl^{9, 17-19}. Therefore, there is great interest to develop alternative biocathodes²⁰. In particular the combination of GOx and HRP²¹ has demonstrated the complete reduction of oxygen into water in the presence of glucose. This bienzymatic alternative is very interesting for the fabrication of biocathodes because these enzymes are both operational under physiological conditions and resistant towards inhibitors¹⁸. The process principle is based on the initial enzymatic reduction of oxygen to H₂O₂ by GOx during glucose oxidation, while H₂O₂ is then further electro-enzymatically reduced to water by adjacent HRP. The involved electrons are provided by the electrode and transferred to the HRP's heme center. This bienzymatic biocathode showed increased performance due to the synergy between the high

surface area of carbon nanotubes (CNT)-modified graphite electrode and the high turnover of these enzymes immobilized thereupon. Furthermore, this technique has to rely on the efficient wiring of HRP in order to ensure a high overpotential for the hydrogen peroxide reduction reaction.

However, the aforementioned electrode designs lack sufficient stability and their performance still lags behind existing multicopper enzyme biocathodes. A major challenge in the development of biofuel cells using such bienzymatic cathodes is to eliminate parasitic side reactions caused by H_2O_2 which can reduce the performance of the said biocathode²² or provoke unwanted toxicity issues²³.

Recent strategies have been attempted to optimize the synergistic effect between these two enzymes in order to increase their performance in terms of current density and onset potential. Co-adsorption of GOx and HRP on double-walled carbon nanotube (DWCNT)-based electrodes²³ or their non-covalent immobilization on CNT using boronic acid¹⁸ was attempted. To date, all bienzyme modified electrode studies were performed on systems where enzymes were directly wired to the electrode.

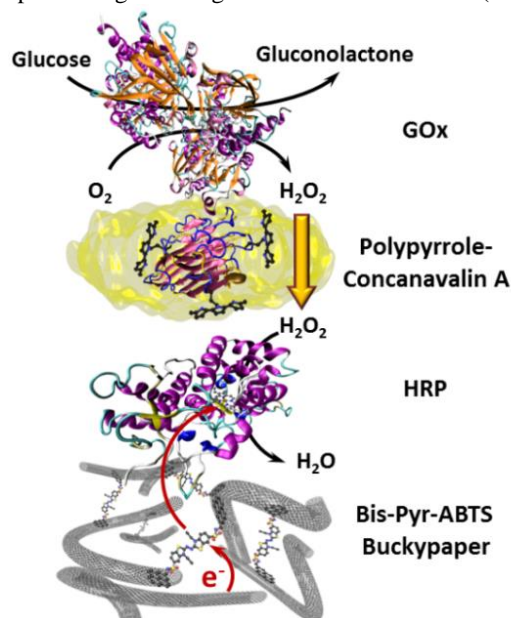
In fact, even though direct electron transfer can provide optimal output voltages, mediated electron transfer can drastically increase the energy conversion yields leading to clearly improved current densities²⁴. Confining enzymes together with their corresponding redox mediator in a highly conducting, porous matrix could considerably enhance the electron transfer and optimize the mass transport of the related substrates. Furthermore, this problem remains one of the key issues in the development of biocathodes in terms of their operational ability under physiological conditions.

In this context, the main strategy herein, focused on the enzyme immobilization technique for the bienzymatic HRP-GOx system in order to maximize the current density and minimize overpotential via mediated electron transfer.

We have proposed to electrogenerate controlled films using pyrrole while combining them with the recognition properties of concanavalin A towards glycosylated proteins like GOx. The electropolymerization of pyrrole groups enables to form a conductive polymer at the surface of the electrode. Polypyrrole favors entrapment of biomolecules such as HRP, while concanavalin A provides an anchor for glycosylated biomolecule immobilization by bioaffinity interactions. Another key advantage of this design is that immobilizing a glycoenzyme through its carbohydrate moiety has no effect on its catalytic properties. The recognition site is generally located in areas that are not involved in enzymatic activity, and hence the enzymes can retain their activity even when their carbohydrate regions are functionalized.

A freestanding redox-buckypaper (BP), reinforced by a cross linking redox mediator pyrene-modified 2,2'-Azino-bis(3-ethylbenzothiazoline-6-sulfonic acid) (Bis-Pyr-ABTS)²⁵, was used as the conductive platform for the immobilization of HRP and GOx. While ABTS enables the mediated electronic communication between HRP and the flexible BP. HRP is further immobilized by electro-polymerization of a pyrrole-

modified concanavalin A layer which then allows the biocompatible high loading immobilization of GOx (scheme 1).



Scheme 1: Sketch of the biocathode functioning based on bis-pyrrole-ABTS BP after adsorption of HRP and subsequent electropolymerization of pyrrole-concanavalin A for the immobilization of GOx.

Results and discussions:

The morphology of the BPs was investigated by SEM and 3D confocal microscopy. Typical images are displayed in Figure 1. The BP cross section shows a porous structure with a specific volume equal to $5 \text{ cm}^3 \text{ g}^{-1}$. The fabricated BP shows thicknesses about $120 \mu\text{m}$ for a BP weight of 25 g m^{-2} . Moreover, the BP electrodes exhibit excellent long-term mechanical stability in aqueous solution.

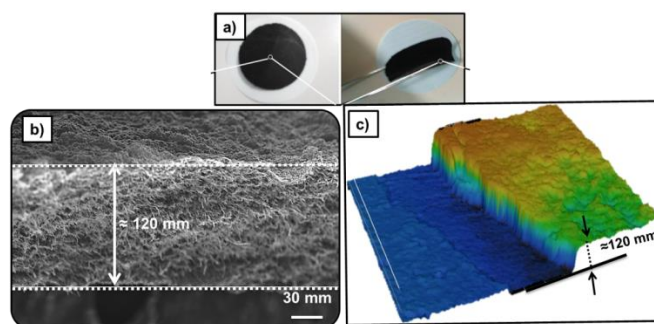


Figure 1. a) Photographs of a as formed BP on a membrane filter and bent with a tweezers. b) SEM image of Bis-Pyr-ABTS BP's cross section. c) Confocal image of Bis-Pyr-ABTS BP.

The electrochemical behavior of Bis-Pyr-ABTS BP/HRP based cathodes was investigated in presence of increasing concentration of H_2O_2 to examine the catalytic H_2O_2 reduction

via mediated electron transfer (MET) and to verify their chloride-tolerance in the presence of 140 mM NaCl.

The Bis-Pyr-ABTS BPs were incubated in a phosphate buffer saline solution (PBS) (0.1 M) containing HRP (5 mg mL⁻¹) and kept at 4 °C overnight to insure efficient adsorption thereof.

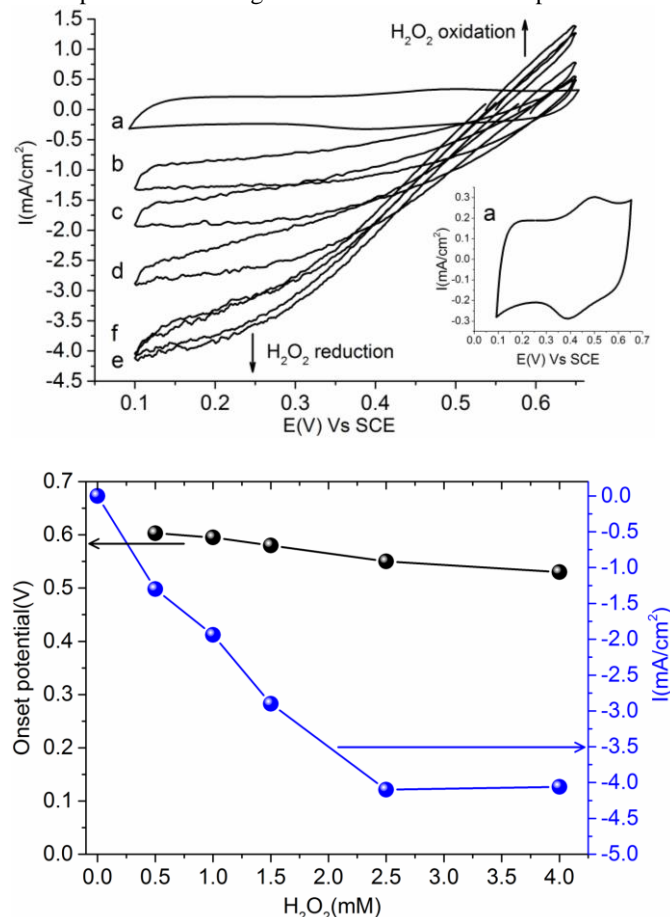


Figure 2. A) Electrode responses of Bis-Pyr-ABTS BP/HRP in the presence of (a) 0, (b) 0.50, (c) 1.0, (d), (e) 2.50 and (f) 4.0 mM H₂O₂ and (inset) electrode responses of Bis-Pyr-ABTS BP/HRP in the presence of 0 mM H₂O₂. (Measurements were performed in 0.1 M PBS (pH 7.4) solution under a nitrogen atmosphere. Potentials are reported versus SCE. Scan rate: 2 mV.s⁻¹. B) Plot of the onset potential (black axis) and evolution of the catalytic current (blue axis) recorded at the Bis-Pyr-ABTS BP/HRP electrodes towards H₂O₂ concentration.

Figure 2A displays the cyclic voltammograms of these biocathodes in the presence and absence of H₂O₂. In absence of H₂O₂, the resulting cyclic voltammograms reveal a reversible peak system characteristic of the one-electron oxidation of ABTS at $\Delta E_{1/2} = +0.46$ V vs. SCE (Fig. 2A inset). It clearly appears that the presence of H₂O₂ induces the appearance of a cathodic current reflecting the H₂O₂ reduction by MET. As expected, upon addition of increasing amounts of H₂O₂, the catalytic cathodic current increases continuously reaching a maximum current density of $-4.1 (\pm 0.2)$ mA cm⁻² at 2.5 mM of H₂O₂. At H₂O₂ concentration higher than 2.5 mM, we observed

the appearance of an oxidative current at a potential higher than 0.5 V. The latter is attributed to the direct oxidation of H₂O₂ at the CNT electrode.

Figure 2B shows the current response of the Bis-Pyr-ABTS BP/HRP cathode as a function of H₂O₂ concentration. The shape of the calibration curve with a linear part and a pseudo plateau at saturating substrate conditions indicates a typical enzymatic dependence.

The onset potential of $0.6 (\pm 0.01)$ V for the reduction of H₂O₂ with Bis-Pyr-ABTS BP/HRP is relatively stable and even more positive compared to oxygen reduction by high-potential BOD^{26, 27} and laccases^{28, 29}. The observed high-potential H₂O₂ reduction current density is slightly reduced at higher H₂O₂ concentration, which is likely due to the concomitant H₂O₂ oxidation at the CNT electrode surface.

As far as we know, this value of onset potential for the electrocatalytic reduction of H₂O₂ is one of the highest, in comparison to those of other reported studies using HRP for H₂O₂ reduction^{16, 27, 29}. As can be seen in Figure 2B, the biocathode shows high onset potential values of $0.60 (\pm 0.01)$ V vs. SCE. Table 1 summarizes the current density and onset potential of this work in comparison with the values described in other reports using HRP as biocathode catalyst.

Table 1: Comparison of the performance of HRP biocathodes for H₂O₂ reduction via DET conditions with the presented Bis-Pyr-ABTS BP/HRP electrode

Ref.	conditions	Electron Transfer	Onset _{max}	I _{max} saturation
181716 151413 121110 ⁹⁸	0.1 M PBS at pH 7.4	DET	+0.43 V	196 μ A cm ⁻² at 0.8 mM
²³	0.1 M PBS at pH 7.4	DET	+0.38 V	120 μ A cm ⁻² at 1 mM
²²	67 mM PB at pH 7.0	DET	+0.47 V	800 μ A at 1 mM
³⁰	0.1 M PB at pH 6.0	DET	+0.62 V	1.2 mA cm ⁻² at 5 mM
This work	0.1 M PBS at pH 7.4	MET	+0.60 V	4.1 mA cm ⁻² at 2.5 mM

The observed high efficiency of electrocatalytic reduction of the Bis-Pyr-ABTS BP/HRP cathodes compared to similar setups with DET is attributed to the presence of ABTS, which might enhance the electron transfer between the electrode surface and the active center of the redox enzyme. This effect may considerably minimize the parasitic oxidation of H₂O₂ on the electrode, which is the major limitation of the use of this system.

A very important drawback in the use of enzymatic cathodes, such as those based on laccases as biocatalysts in biofuel cells, comes from their poor performance at neutral pH and the inhibition effect of anions such as chloride. Hence, we

investigated the catalytic performance of Bis-Pyr-ABTS BP/HRP for H_2O_2 reduction under physiological conditions, namely in presence of chloride. After an initial stabilization of the catalytic cathodic current, the injection of NaCl (140 mM) after 700 s does not induce any inhibitory effect, the catalytic current remaining stable for 700 s (Figure 3). For comparison, Figure 3 shows an example of chrono-amperometric measurements under similar inhibiting conditions for a previously-reported Bis-Pyr-ABTS BP containing laccase²⁵. In contrast to HRP based cathodes, this laccase cathode undergoes a rapid and partial decrease of the electrocatalytic current for oxygen reduction over time (a decrease of 22% after 8 min).

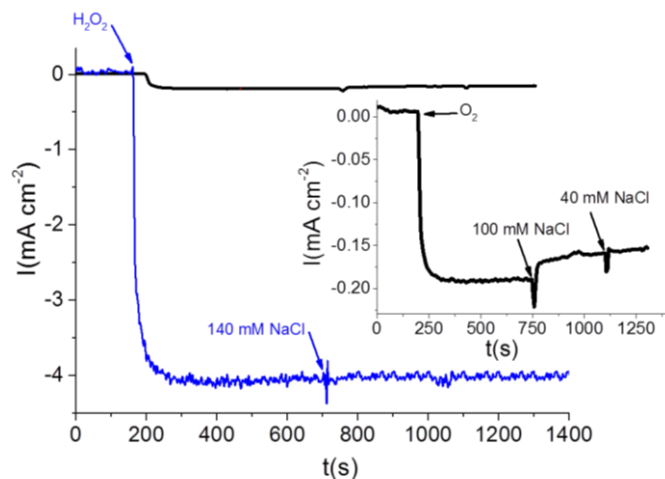


Figure 3. Evolution of the current density for reduction of O_2 or H_2O_2 at 0.1 V versus SCE recorded at (blue) Bis-Pyr-ABTS BP/HRP cathode and at (black and inset) a Bis-Pyr-ABTS BP/ Laccase cathode in 0.1 M PB (pH 7.4). Measurements were performed (blue) in PB with injection of H_2O_2 (2.5 mM) after 170s then NaCl (140 mM) after 700 s or (black and inset) under a nitrogen atmosphere saturated with O_2 after 200 s and with successive increments of NaCl concentration (100 and then 40 mM after 750 and 1120 s).

We engineered a bienzymatic biocathode for oxygen reduction via the catalytic cascade reactions using combined HRP and GOx catalysts. GOx catalyzes the oxidation of glucose to gluconic acid with the concomitant generation of H_2O_2 . The biocatalytically-generated H_2O_2 from the consumption of dissolved O_2 then acts as the oxidizer for HRP. Electrons, which reduce H_2O_2 , are transferred from the electrode surface to the HRP by ABTS. Our approach consists in the GOx immobilization on a Bis-Pyr-ABTS BP/HRP electrode previously modified by an electrogenerated polypyrrole concanavalin A film.

The possibility to form a polymeric proteinaceous film not only allows the entrapment of HRP but also acts as a binding bridge between BP and glycosylated enzymes like GOx.

The polypyrrole-Con A film was generated at Bis-Pyr-ABTS BP/HRP by controlled potential electrolysis ($E_{\text{applied}} = +0.65$ V versus SCE, $Q = 10 \text{ mC cm}^{-2}$) in PBS. The resulting Bis-Pyr-

ABTS BP/HRP Polypyrrole-Con A electrodes were washed with PBS and then incubated at room temperature in GOx solution (5 mg/mL in PB, pH 7.4) for 4h. Finally, unbound GOx was eliminated by washing with PB (0.1 M, pH 7.4).

In order to determine the capacity of such a bienzymatic system in its reduction of O_2 , its response to glucose was studied. Figure 4A shows the cyclic voltammograms recorded at a Bis-Pyr-ABTS BP/HRP/Polypyrrole-Con A/GOx electrode in 0.1 M PBS (pH 7.4) containing various glucose concentrations under an air atmosphere. In the absence of glucose and presence of O_2 , any catalytic current is observed at the Bis-Pyr-ABTS BP/HRP/Polypyrrole-Con A/GOx electrode. In contrast, in the presence of glucose and O_2 , the biocathode exhibits a remarkable catalytic current peak with a current density of about $-1.1 (\pm 0.1) \text{ mA cm}^{-2}$ at 0.1 V. The cyclic voltammograms exhibit an onset potential of $+0.6 (\pm 0.01) \text{ V}$ for the electrocatalytic H_2O_2 reduction. The observed cathodic current density indicates the efficient conversion of the enzymatically generated H_2O_2 to water, where the involved electrons are transferred from the electrode to HRP via ABTS. Such observations indicate that Bis-Pyr-ABTS BP/HRP/Polypyrrole-Con A/GOx possesses a high electrocatalytic activity toward H_2O_2 reduction, and by consequence, towards O_2 reduction.

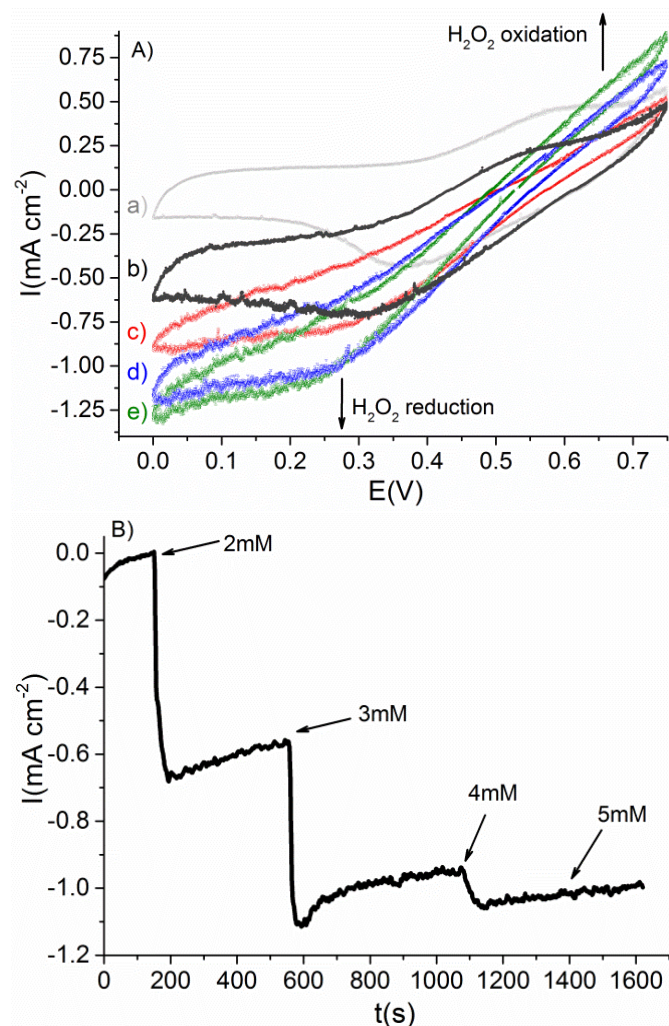


Figure 4. A) Cyclic voltammograms of Bis-Pyr-ABTS BP/HRP/Polypyrrole-Con A/GOx biocathodes in the absence (a) or presence of (b) 2, (c) 3, (d) 4 and (e) 5 mM glucose B) Evolution of the H_2O_2 reduction current density upon addition of glucose recorded at this biocathode poised at 0.1 V versus SCE. Measurements were performed in 0.1 M PBS (pH 7.4) solution under an air atmosphere; scan rate: $2 \text{ mV} \cdot \text{s}^{-1}$.

Figure 4B shows the amperometric responses at 0.1 V after addition of defined amounts of glucose revealing an increase of the catalytic current for increased concentration of glucose from 1 to 5 mM and they then stabilize at higher concentrations. The catalytic current of the biocathode reaches saturation at 4–5 mM glucose concentration. This may be ascribed to a saturation of the peroxidase electroactivity.

To evaluate the long-term stability of the biocathode, the current density for glucose (5 mM) was periodically recorded by performing one-hour discharge at 0.1 V for 15 days. The biocathode still delivered $0.7 (\pm 0.1) \text{ mA cm}^{-2}$ after 15 days (Figure 5), which represents 64 % of its initial electrocatalytic activity and constitutes the highest lifetime reported until now for a bienzymatic cathode using HRP.

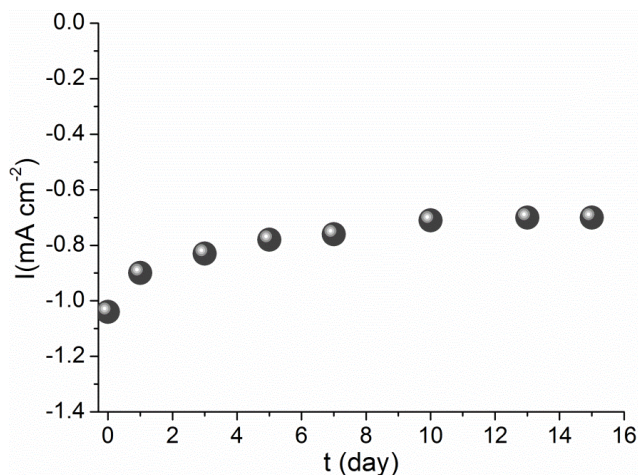


Figure 4: Operational stability of the Bis-Pyr-ABTS-BP/HRP/Polypyrrole-Con A/GOx cathode. Measurements were performed in 0.1 M PBS (pH 7.4) solution under air atmosphere at 0.1 V vs SCE.

Conclusions

These results demonstrate that these bienzymatic BP electrodes exhibit high current density for oxygen reduction with low overpotentials and excellent stability over weeks. This proof of concept demonstrates that redox BP/HRP/Polypyrrole-Con A/GOx can advantageously replace the conventional biocathodes based on multicopper enzymes that are employed in biofuel cells. Taking into account their possibility to operate under physiological conditions, it is expected that such bienzyme cathodes will be useful for the development of implantable biofuel cells, while other systems can also benefit of such set-ups.

Acknowledgements

The authors thank the platform “functionalization of surfaces and transduction” of the scientific structure “Nanobio campus” for providing facilities. The authors also thank the ANR Investissements d’avenir-Nanobiotechnologies 10-IANN-0-02 program, the PICS CNRS 06344 program and the Labex ARCANÉ (ANR-11-LABX-0003-01) for partial financial support. This research is conducted by NTU-HUJ-BGU Nanomaterials for Energy and Water Management Programme under the Campus for Research Excellence and Technological Enterprise (CREATE), that is supported by the National Research Foundation, Prime Minister’s Office, Singapore.

Notes and references

^a Univ. Grenoble Alpes, DCM UMR 5250, F-38000 Grenoble, France CNRS, DCM UMR 5250, F-38000 Grenoble, France

^b CREATE, School of Material Science and Engineering, Nanyang Technology University, Nanyang Avenue, 639798, Singapore

^c The Department of Biotechnology Engineering, The National Institute for Biotechnology in the Negev and the Ilse Kats Institute for Nanoscale Science and Technology, The Ben Gurion University of the Negev, Beer Sheva, 84105, Israel

†Electronic Supplementary Information (ESI) available: [details of any supplementary information available should be included here]. See DOI: 10.1039/b000000x/

1. S. Cosnier, A. Le Goff and M. Holzinger, *Electrochem. Commun.*, 2014, **38**, 19–23.
2. M. Rasmussen, R. E. Ritzmann, I. Lee, A. J. Pollack and D. Scherson, *J. Am. Chem. Soc.*, 2012, **134** 1458–1460.
3. L. Halámková, J. Halámek, V. Bocharova, A. Szczupak, L. Alfonta and E. Katz, *J. Am. Chem. Soc.*, 2012, **134**, 5040–5043.
4. A. Szczupak, J. Halámek, L. Halámková, V. Bocharova, L. Alfonta and E. Katz, *Energy Environ. Sci.*, 2012, **5**, 8891–8895.
5. K. MacVittie, J. Halamek, L. Halamkova, M. Southcott, W. D. Jemison, R. Lobel and E. Katz, *Energy Environ. Sci.*, 2013, **6**, 81–86.
6. P. Cinquin, C. Gondran, F. Giroud, S. Mazabrard, A. Pellissier, F. Boucher, J.-P. Alcaraz, K. Gorgy, F. Lenouvel, S. Mathé, P. Porcu and S. Cosnier, *PLoS ONE*, 2010, **5**, e10476.
7. F. C. P. F. Sales, R. M. Iost, M. V. A. Martins, M. C. Almeida and F. N. Crespilho, *Lab on a Chip*, 2013, **13**, 468–474.
8. H. Cheng, P. Yu, X. Lu, Y. Lin, T. Ohsaka and L. Mao, *Analyst*, 2013, **138**, 179–185.
9. A. Zebda, S. Cosnier, J.-P. Alcaraz, M. Holzinger, A. Le Goff, C. Gondran, F. Boucher, F. Giroud, K. Gorgy, H. Lamraoui and P. Cinquin, *Sci. Rep.*, 2013, **3**, 1516.
10. J. A. Castorena-Gonzalez, C. Foote, K. MacVittie, J. Halámek, L. Halámková, L. A. Martinez-Lemus and E. Katz, *Electroanalysis*, 2013, **25**, 1579–1584.
11. T. Miyake, K. Haneda, N. Nagai, Y. Yatawaga, H. Onami, S. Yoshino, T. Abe and M. Nishizawa, *Energy & Environmental Science*, 2011, **4**, 5008–5012.
12. S. Shleev, A. Jarosz-Wilkolazka, A. Khalunina, O. Morozova, A. Yaropolov, T. Ruzgas and L. Gorton, *Bioelectrochemistry*, 2005, **67**, 115–124.
13. A. Zebda, C. Gondran, A. Le Goff, M. Holzinger, P. Cinquin and S. Cosnier, *Nature Communications*, 2011, **2**, 370.
14. N. Mano, H.-H. Kim and A. Heller, *The Journal of Physical Chemistry B*, 2002, **106**, 8842–8848.
15. N. Mano and A. Heller, *J. Electrochem. Soc.*, 2003, **150**, A1136–A1138.
16. N. Mano, J. L. Fernandez, Y. Kim, W. Shin, A. J. Bard and A. Heller, *J. Am. Chem. Soc.*, 2003, **125**, 15290–15291.
17. S. C. Barton, M. Pickard, R. Vazquez-Duhalt and A. Heller, *Biosens. Bioelectron.*, 2002, **17**, 1071–1074.
18. B. Reuillard, A. Le Goff, M. Holzinger and S. Cosnier, *Journal of Materials Chemistry B*, 2014, **2**, 2228–2232.
19. E. Katz and K. MacVittie, *Energy & Environmental Science*, 2013, **6**, 2791–2803.
20. R. A. S. Luz, A. R. Pereira, J. C. P. de Souza, F. C. P. F. Sales and F. N. Crespilho, *ChemElectroChem*, 2014, **1**, 1751–1777.
21. W. Jia, C. Jin, W. Xia, M. Muhler, W. Schuhmann and L. Stoica, *Chem. Eur. J.*, 2012, **18**, 2783–2786.
22. W. Jia, S. Schwaborn, C. Jin, W. Xia, M. Muhler, W. Schuhmann and L. Stoica, *Phys. Chem. Chem. Phys.*, 2010, **12**, 10088–10092.
23. C. Agnès, B. Reuillard, A. Le Goff, M. Holzinger and S. Cosnier, *Electrochem. Commun.*, 2013, **34**, 105–108.
24. B. Reuillard, A. Le Goff, C. Agnès, M. Holzinger, A. Zebda, C. Gondran, K. Elouarzaki and S. Cosnier, *Phys. Chem. Chem. Phys.*, 2013, **15**, 4892–4896.
25. M. Bourourou, K. Elouarzaki, M. Holzinger, C. Agnes, A. Le Goff, N. Reverdy-Bruas, D. Chaussy, M. Party, A. Maaref and S. Cosnier, *Chemical Science*, 2014, **5**, 2885–2888.
26. N. Mano and L. Edembe, *Biosens. Bioelectron.*, 2013, **50**, 478–485.
27. L. Hussein, G. Urban and M. Kruger, *Phys. Chem. Chem. Phys.*, 2011, **13**, 5831–5839.
28. A. Le Goff, M. Holzinger and S. Cosnier, *Cell. Mol. Life Sci.*, 2015, **72**, 941–952.
29. L. Hussein, S. Rubenwolf, F. von Stetten, G. Urban, R. Zengerle, M. Krueger and S. Kerzenmacher, *Biosens. Bioelectron.*, 2011, **26**, 4133–4138.
30. M. Varničić, K. Bettenbrock, D. Hermsdorf, T. Vidaković-Koch and K. Sundmacher, *RSC Advances*, 2014, **4**, 36471–36479.